

Statistical analysis of winter ozone events

Marc L. Mansfield · Courtney F. Hall

Received: 1 May 2013 / Accepted: 1 September 2013 / Published online: 26 September 2013
© Springer Science+Business Media Dordrecht 2013

Abstract We have developed quadratic regression models that predict the daily ozone concentration in either the Uintah Basin (UB) of Utah, USA, or the Upper Green River Basin (UGRB) of Wyoming, USA. Sites selected for study are ozone stations near the towns of Ouray, Utah, in the UB and Boulder, Wyoming, in the UGRB. Input data for the UB model are daily values of lapse rate, snow depth, solar angle, temperature, and the number of consecutive days under inversion conditions. The UGRB model also requires the wind speed. Standard errors are 10 and 5 ppb for the UB and the UGRB, respectively. The models have been optimized to predict seasonal exceedances of the National Ambient Air Quality Standard (NAAQS), i.e., the number of times each season that the daily maximum in the eight-hour running average exceeds 75 ppb, and they perform in this regard to an accuracy of ± 1 day. (However, Ouray is not at this time a regulatory site for judging compliance with federal law.) We predict that any given winter will be NAAQS compliant with 44 % odds in the UB and with 60 % odds in the UGRB. We have estimated the ozone production for each winter in the UB since 1950, under the assumption that precursor emissions are at modern values.

Keywords Winter ozone · Uintah Basin, Utah · Upper Green River Basin, Wyoming · Quadratic regression

Electronic supplementary material The online version of this article (doi:10.1007/s11869-013-0204-0) contains supplementary material, which is available to authorized users.

M. L. Mansfield (✉) · C. F. Hall
Bingham Research Center, Utah State University,
320 N Aggie Boulevard, Vernal, UT 84078, USA
e-mail: marc.mansfield@usu.edu
URL: rd.usu.edu

C. F. Hall
e-mail: courtney.hall@usu.edu

Introduction

Tropospheric ozone events occur almost exclusively in large cities in summer because, first, cities have elevated concentrations of anthropogenic ozone precursors and, second, because the summer season provides abundant solar energy to power ozone formation. However, ozone concentrations high enough to produce numerous exceedances of the 75-ppb 8-h-average National Ambient Air Quality Standard (NAAQS) have been observed in winter in two rural areas of the Western United States, the Upper Green River Basin (UGRB) of Sublette County, Wyoming, and the Uintah Basin (UB) of Duchesne and Uintah Counties, Utah (see Fig. 1). (“Uinta” is a common alternate spelling for “Uintah.”) Both regions are prone to intense thermal inversions in winter, both often have surface snow cover persisting for three or more months, and both are regions of intense fossil fuel extraction (Schnell et al. 2009; Martin et al. 2011).

Ozone formation in these two basins is known to correlate strongly with both thermal inversions and snow cover. A conceptual model that has strong support among researchers holds that persistent (i.e., multiday) thermal inversions with tight boundary layers permit accumulation and concentration of ozone precursors, while the increased surface albedo of snow intensifies the amount of solar energy available for ozone production (Stoeckenius and Ma 2010). The actinic flux tables given by Finlayson-Pitts and Pitts (2000) confirm that actinic flux in the snow-covered Uintah Basin at midday of the winter solstice is very close to that of the Los Angeles Basin at the summer solstice. Because both the UGRB and the UB are rural (populations of about 10,000 and 52,000, respectively) and because the only heavy industry in either is fossil fuel extraction, this industry is believed to be primarily responsible for the generation of the requisite ozone precursors.

Since ozone production in these basins requires both thermal inversions and snow cover, some winters are worse for

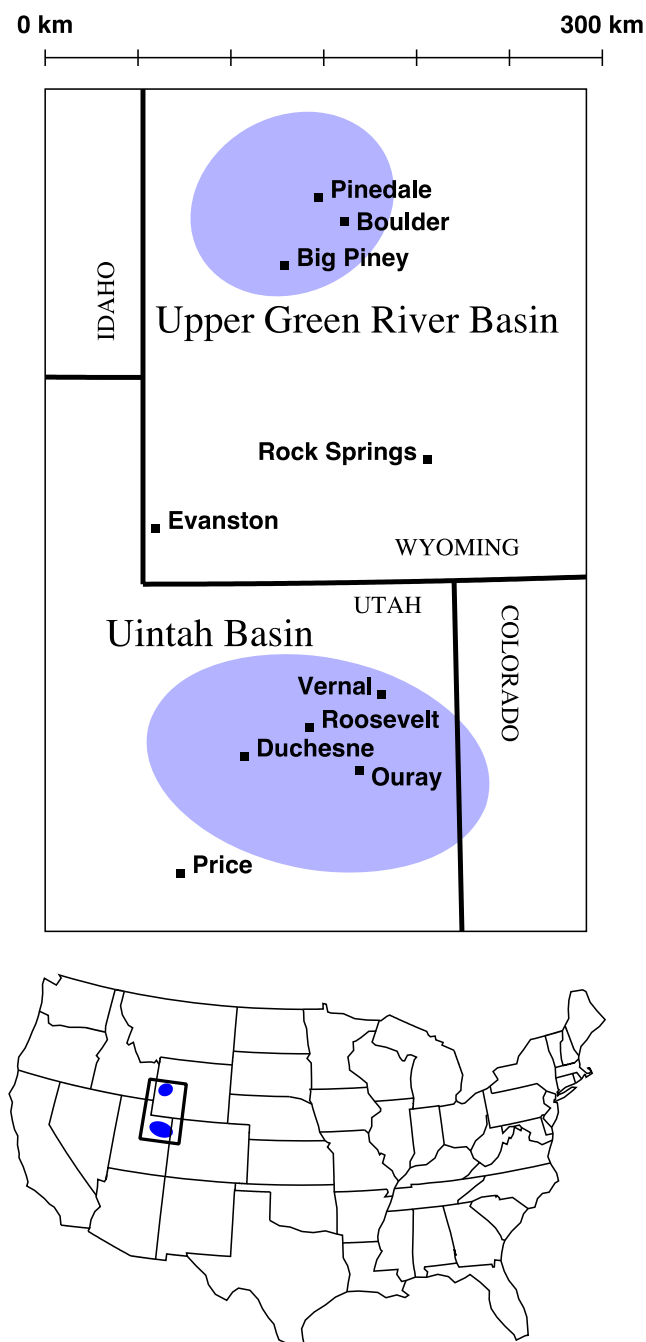


Fig. 1 Map showing the locations of the Upper Green River Basin in Wyoming and the Uintah Basin in Utah. The floors of the Upper Green and the Uintah Basins are at respective elevations of about 1,900 and 1,400 m

ozone than others. In the UB, there were many ozone exceedances during two winters with abundant snow cover, namely, 2009–2010 and 2010–2011, but none during the 2011–2012 winter, which lacked snow. No measurements exist for prior winters. The UGRB shows similar fluctuations from year to year, with 2004–2005, 2007–2008, and 2010–2011 being relatively high for ozone. One purpose of the study reported here is to use historical climate data to better

understand the likelihood that any given winter season will exhibit elevated ozone concentrations.

We employed ozone data from stations near the towns of Ouray, Utah, in the UB and Boulder, Wyoming, in the UGRB. These stations were selected either because they had longer time-series data or because they tend to show higher ozone concentrations than others in their respective basins. However, the Ouray station is nonregulatory; the Environmental Protection Agency (EPA) is not currently using it to judge compliance with the NAAQS. This explains why it is possible for us to state in this paper an exceedance number in any given season that differs slightly from the regulatory value employed by the EPA.

Based on this study, we estimate that at current precursor levels and with current climate trends, winters in the UB have about 44 % odds of being NAAQS compliant, and about 14 % odds of being as bad or worse for ozone than the 2009–2010 season, which had around 40 exceedances of the NAAQS standard and at the time of this study, was the worst ozone season on record in the UB. (At this writing, the 2012–2013 season is now the worst season on record.) We also predict that winters in the UGRB are compliant about 60 % of the time.

We make these predictions using a multivariate regression analysis that is described below. The analysis uses a number of daily meteorological variables, as well as the daily ozone maximum, taken over all seasons for which ozone data are available (three and eight seasons, respectively, for the UB and the UGRB). Together, these constitute the “training” or the “calibration” dataset, with ozone concentrations acting as the dependent variable and all others acting as independent variables. The regression coefficients can then be used to estimate daily ozone concentrations as a function of the independent variables, even in the absence of ozone measurements. The standard errors between measured and predicted ozone are about 10 and 5 ppb, respectively, in the UB and the UGRB. Furthermore, in every winter for which sufficient data are available and in both basins, our analysis always predicts the correct number of exceedances per season to within ± 1 day.

Other important contributions of this study are (1) the development of a practical technique for characterizing thermal inversions in the absence of sonde data and (2) an appraisal of the sensitivity of winter ozone levels to a number of meteorological variables.

McVehil-Monnett and Inc. (2011)) have also performed a statistical study of winter ozone conditions in the UGRB. Their analysis, although not based on regression, reached a number of conclusions similar to ours.

A previous, unpublished account of this research, limited to the UB and employing slightly different versions of the regression models, may be found in Mansfield and Hall (2013). Since then, there have been a few minor adjustments to the models, but the results reported here are in qualitative agreement with that report.

Model description: quadratic regression

Since standards of ozone compliance are based on daily ozone values, usually the daily maximum in the 8-h running average, we have found it convenient to employ daily values of all the variables, usually using a daily maximum or a daily average. See below for the complete specifications of the daily variables employed. The value of an independent variable will be denoted $x_{j\alpha}$, which represents the value of variable j on day α . (Our subscripting convention in this paper is that Roman indices specify the type of variable while Greek indices specify the day.) The dependent variable will be denoted y_α , which will always represent the daily maximum in the 8-h running average ozone concentration at some monitoring site on day α .

The regression model consists of the following formula:

$$\bar{y}_\alpha = A + \sum_j B_j x_{j\alpha} + \sum_{j \leq k} C_{jk} x_{j\alpha} x_{k\alpha} \quad (1)$$

where \bar{y}_α designates the ozone concentration on day α as predicted by the model. The coefficients A , B_j , and C_{jk} are adjusted to minimize the following function:

$$S = \sum_\alpha W_\alpha (\bar{y}_\alpha - y_\alpha)^2 \quad (2)$$

The W_α terms are weight factors that increase the flexibility of the model and whose assignment is explained below. The overall quality of fit can be gauged either with the standard deviation

$$\sigma = \left[\frac{1}{N} \sum_\alpha (\bar{y}_\alpha - y_\alpha)^2 \right]^{1/2} \quad (3)$$

where N is the total number of days in the calibration set or the standard error

$$\varepsilon = \frac{1}{N} \sum_\alpha |\bar{y}_\alpha - y_\alpha| \quad (4)$$

Minimization of S with respect to A , B_j , and C_{jk} is achieved through a straightforward Gauss–Jordan elimination.

Equation (1) is an example of a quadratic regression. Linear regressions, for which the quadratic terms in Eq. (1) are not included are, of course, very popular. We decided to include quadratic terms to enhance the flexibility of the model. For example, the quadratic terms allow for synergistic interactions among the variables.

The model is operated in either a “calibration” mode or a “prediction” mode. The “calibration set” is a set of days for

which all independent variables, $X_{j\alpha}$, and all dependent variables, y_α or the ozone concentrations, are known, and calibration consists of determining the coefficients A , B_j , and C_{jk} that optimize Eq. (2) over all days in the set. The “prediction set” is a set of days for which all $X_{j\alpha}$ are known. The prediction mode consists of using the coefficients obtained during calibration to predict ozone concentrations for every day in the prediction set. Because ozone measurements are not used in prediction, the prediction set is generally larger than the calibration set.

In particular, we include in the prediction set days that predate the beginning of winter ozone measurements in these basins, going back to 1950 in the UB and 1997 in the UGRB. (We started this study with historical data to the 1990s in both basins, but then decided to extend the UB study for an additional 40 years, in order better to test for long-range data trends.) In so doing, we are not implying that past ozone precursor concentrations are comparable to their contemporary levels. Rather, the objective is to use historical climate data to determine the likelihood that a given winter season, under typical present-day precursor concentrations, would develop high ozone levels.

Meteorological variables

In this section, we describe the meteorological variables used in the model, including definitions and sources. As mentioned above, the model is based on daily values of the variables, so here we also explain how a daily value for each variable has been defined. “Acronyms for variables” describes our abbreviation system for variable names. “Eight-hour ozone concentrations,” “Basin lapse rate, basin temperature, and consecutive days under inversion,” “Average basin snow depth,” “Midday solar angle,” and “Daily average wind speed, relative humidity, and barometric pressure” describe in detail how each variable was assigned. Table 1 lists statistical properties of the variables used.

Acronyms for variables

For convenience, we employ acronyms to designate all meteorological variables. The complete acronym consists of two parts. The first part codes for the type of variable, while the second codes for the applicable basin. For example, LR:UB will be used to designate the lapse rate defined for the Uintah Basin.

Eight-hour ozone concentrations

Running eight-hour average ozone concentrations (O8) at sites near the towns of Ouray, Utah, in the UB and Boulder, Wyoming, in the UGRB, were obtained from a website

Table 1 The ranges, means, and standard deviations of the various variables in the calibration sets of the various models

	Minimum	Maximum	Mean	SD
Uintah Basin datasets				
O8:UB (ppb)	21	139	64	26
LR:UB (K/km)	−21	14	0	8
SD:UB (mm)	0	370	149	105
SA:UB (°)	42	64	57	6
BT:UB (°C)	−18	14	−1	7
CDI:UB (days)	0	43	5	10
WS:UB (m/s)	0.2	7.4	1.2	1.0
RH:UB (%)	29	97	74	12
BP:UB (bar)	0.816	0.854	0.839	0.007
Upper Green River Basin datasets				
O8:UGRB (ppm)	22	123	50	13
LR:UGRB (m/s)	−68	30	−1	13
SD:UGRB (mm)	46	752	361	150
SA:UGRB (°)	45	66	58	7
BT:UGRB (°C)	−29	14	−2	6
CDI:UGRB (days)	0	8	0.9	1.4
WS:UGRB (m/s)	0	8.6	2.8	1.6
RH:UGRB (%)	37	94	75	9
BP:UGRB (bar)	0.763	0.801	0.785	0.006

maintained by the EPA (2012). The Ouray dataset includes three winter seasons: 2009–2010, 2010–2011, and 2011–2012. No prior measurements exist. The Boulder dataset covers eight winter seasons, beginning with 2004–2005 and ending with 2011–2012. In most cases, the datasets were selected to include the winter period from mid-December to mid-March. Units employed for O8 are parts per billion by volume.

Basin lapse rate, basin temperature, and consecutive days under inversion

A temperature inversion is indicated when the temperature of the atmosphere increases with altitude, and experience indicates that inversions are required for winter ozone formation. Inversions are characterized by the so-called lapse rate (LR) (Seinfeld and Pandis 2006):

$$A = -\frac{dT}{dz} \quad (5)$$

where T represents temperature and z the altitude. By this definition, a negative lapse rate indicates a temperature inversion. Lapse rates are determined by sonde measurements, which are obviously not available day in and day out. Therefore, we developed the following approach to estimate a daily lapse rate for a given basin. Daily temperature data at a set of

meteorological stations from throughout each basin at various altitudes and at all available dates between about 1950 and 2012 (UB) or about 1990 and 2012 (UGRB) were assembled from the database maintained by the Utah Climate Center (2012) (See Online Resource 1 for lists and maps of stations contributing data for this study, and for the selection criteria used to select stations.) For any given date, we construct a least-squares linear correlation between maximum daily temperature and altitude, employing data from all stations reporting a maximum temperature for the day. The LR for any given day is defined operationally as the negative of the slope of the correlation line. Figure 2 shows the linear correlations for four selected days in the UB. The slope is negative on typical summer days, but positive for winter days with inversions. We express LR in Kelvin/kilometer.

The linear-least-squares fit to the temperature–altitude data also permits us to define a daily, basin-wide temperature (BT). We take BT to be the value at which the least-squares line intersects an altitude near the floor (1,400 and 1,900 m, respectively) of the basin. Our units for BT are degrees Celsius.

Because ozone precursor concentrations are expected to accumulate over persistent, multiday inversions, we have introduced the variable consecutive days under an inversion (CDI). The value of $CDI(\alpha)$ is 0 on any day α for which $LR(\alpha)$ (the lapse rate) is positive. If $LR(\alpha)$ (i.e., one day's lapse rate) is negative while $LR(\alpha - 1)$ (i.e., the previous day's lapse rate) is positive, then $CDI(\alpha) = 1$ day. If $LR(\alpha)$ and $LR(\alpha - 1)$ are both negative, then $CDI(\alpha) = CDI(\alpha - 1) + 1$ day.

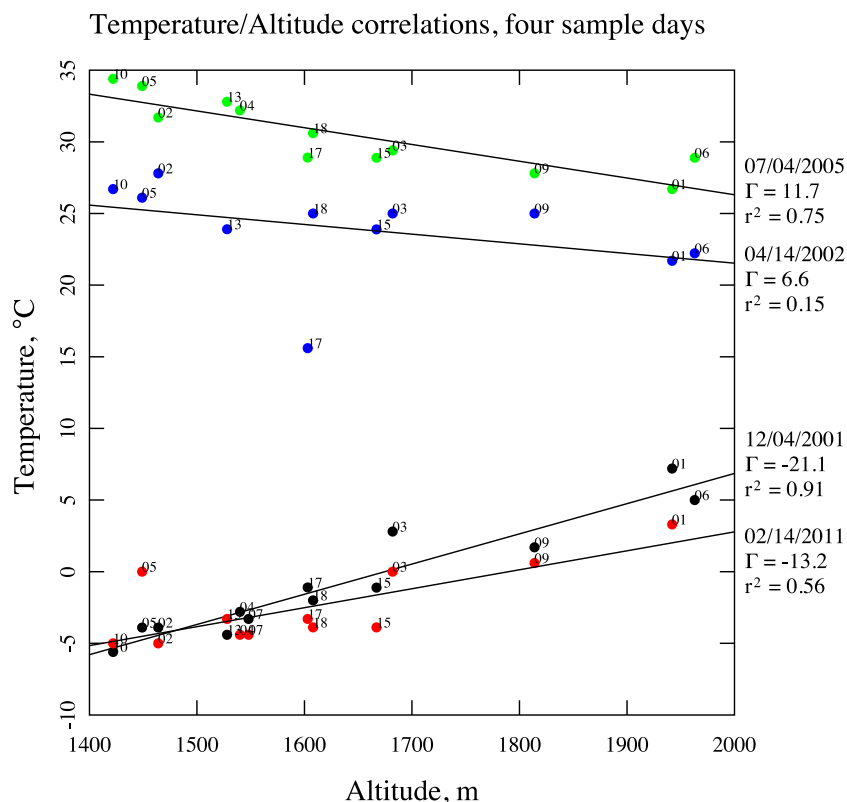
Average basin snow depth

Snow depth (SD) data were also obtained from the Utah Climate Center (2012) using the same stations as for the LR calculation. However, we have found occasional problems with the quality of the data. (For example, one station may report a snow depth of 0 when all others report abundant snow.) Therefore, the following procedure was employed: For any given day, we calculated an average snow depth by averaging over all stations reporting a depth, interpreting “T” (trace) as 10 mm. We then rejected any measurement that fell more than 2 standard deviations away from the mean for the day. After that rejection, a new mean was calculated. Units employed here for SD are millimeters.

Midday solar angle

The solar angle (SA) at its midday extremum was calculated using formulas found in Finlayson-Pitts and Pitts (2000), using coordinates of the towns of Roosevelt, Utah (40.30°, −109.99°) and Boulder, Wyoming (42.719°, −109.753°), for the UB and the UGRB, respectively. We employ units of degrees and observe the convention that 0 and 90° solar angles refer to the zenith and the horizon, respectively.

Fig. 2 Temperature–altitude correlations for four typical days in the Uintah Basin. Each point in the figure is labelled with a number that corresponds to a map and table in the supplementary information. The numerical value of the daily lapse rate in K/km and the r^2 correlation coefficients are also displayed



Daily average wind speed, relative humidity, and barometric pressure

Pre- and post-2005 data for these three variables were obtained from websites maintained by the National Oceanic and Atmospheric Association (NOAA), the Unedited Local Climatological Data (ULCD), and Quality Controlled Local Climatological Data (QCLCD) databases, respectively (NOAA:NCDC 2012). We used the datasets from the Vernal Municipal and the Big Piney-Marbleton Regional Airports, respectively, to represent the UB and the UGRB. The ULCD and QCLCD databases include hourly observations of all three variables, which we averaged to obtain a daily variable. Units employed for wind speed (WS), relative humidity (RH), and barometric pressure (BP) are meters per second, percent, and bars, respectively.

Climatic observations based on the data

Figure 3 shows the average lapse rate on any particular calendar day for both basins. It indicates that thermal inversions are very common in both basins in the winter. It also indicates that winter lapse rates display a higher variability than those of summer.

Figure 4 displays the probability that any given calendar day in the respective basins has snow cover (red, defined

operationally as a day with $SD > 50$ mm), has an inversion (blue, defined operationally as a day with $LR < 0$), or simultaneously has an inversion and snow cover (green). Both actual data and best-fit Gaussian distributions (truncated at 1 for the case of snow cover in UGRB) are displayed. By definition, the green traces in Fig. 4 must lie below the blue and red traces (although this requirement does not extend to the Gaussian fits). The fact that all three lie close together for the UB indicates that snow cover plays an important role in stabilizing inversions there. In the UGRB, on the other hand, we see inversions occurring in the absence of snow cover, in spring or fall, for example. Figures 3 and 4 indicate that January is the peak month in both basins for snow cover and inversions.

Model development and performance, calibration mode

Because daily data are not always available, we are forced to compromise between having a diverse set of independent variables and having a large number of days in the prediction set. To explore optimal trade-offs, we have constructed a few different models of the ozone system of each basin. These models are summarized in Tables 2 and 3. Two of the models, Ouray-8 and Ouray-5, are applicable to the UB, and use ozone concentration measurements from a station near Ouray, Utah. The other three models, Boulder-5, Boulder-6, and Boulder-8, are applicable to the UGRB and refer to an ozone station near

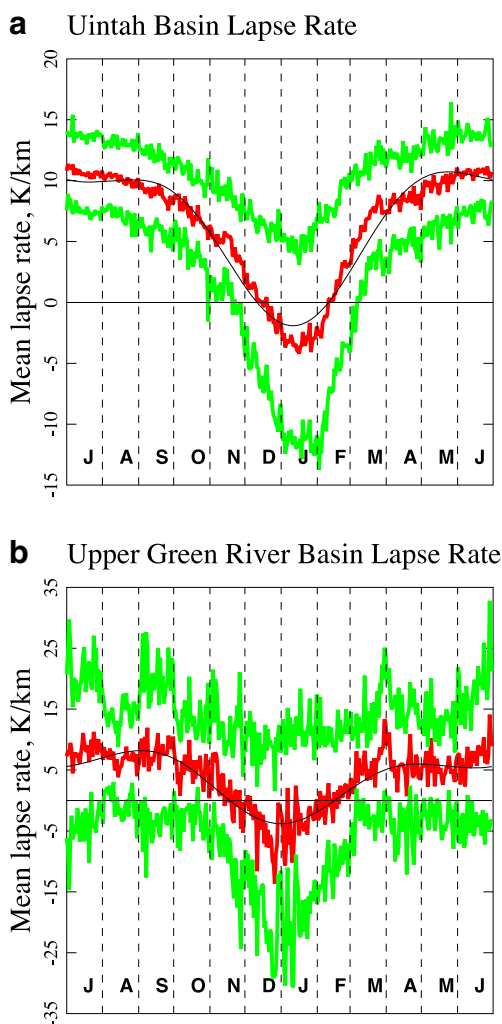


Fig. 3 Average daily lapse rate in the Uintah Basin (a) and the Upper Green River Basin (b). The red traces are the lapse rate itself; the green traces are displaced above and below by one standard deviation. The black curves are a filtered representation of the red trace

Boulder, Wyoming. In each case, the numerical suffix indicates the number of independent variables used by the model. Specifically, Ouray-8 and Boulder-8 use the following eight independent variables: (1) LR, (2) SD, (3) BT, (4) SA, (5) CDI, (6) WS, (7) RH, and (8) BP. Boulder-6 is obtained by dropping RH and BP, and Boulder-5 by also dropping WS. Ouray-5 is obtained from Ouray-8 by dropping RH, BP, and WS. By eliminating certain variables, we are able to expand the prediction set, since, for example, available wind speed data does not extend as far back as available snow depth data. The question, however, is the degree to which the predictive power of the model deteriorates with the omission of certain variables. As explained below, we have determined that Ouray-5 and Boulder-6 are the models of choice for optimizing the trade-off mentioned above.

The weight factors shown in Eq. (2) permit us to apportion greater weights to some days in the calibration set than to

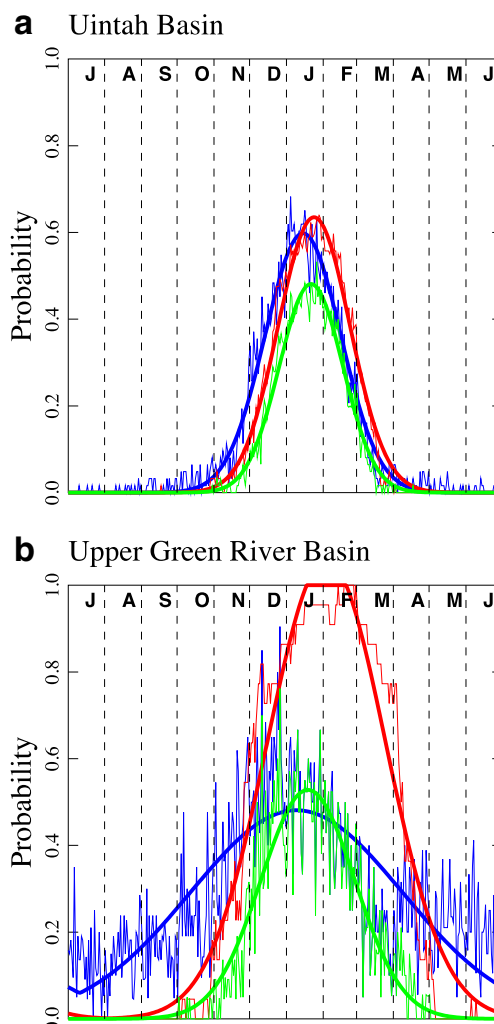


Fig. 4 The probability that a given day in the Uintah Basin (a) and the Upper Green River Basin (b) has mean snow depth >50 mm (red), has negative lapse rate (blue), or simultaneously has both (green). Evaluated over about 60 years for the Uintah Basin and about 20 for the Upper Green River Basin. Also shown are best-fit Gaussian distributions

others. We used the following formula to assign a weight to each day in each calibration set:

$$W_{\alpha} = \left(\frac{y_{\alpha}}{\hat{c}} \right)^p \tag{6}$$

As explained above, y_{α} is the ozone concentration for day α . \hat{c} is the unit concentration of 1 ppb—its presence in Eq. (6) is a formality that renders W_{α} dimensionless—and p is an adjustable exponent. Selecting $p > 0$ imparts greater weights to high-ozone days and vice versa. The value of p was adjusted (by trial and error) to optimize the agreement between the actual and the predicted number of days per season that the NAAQS ozone standard of 75 ppb is exceeded. The p values employed in each model are given in Table 2.

The regression coefficients for each model are given in Online Resource 2.

Table 2 Variable sets and other characteristics of each of the models

	Ouray-8	Ouray-5	Boulder-8	Boulder-6	Boulder-5
Dependent variable	O8:UB	O8:UB	O8:UGRB	O8:UGRB	O8:UGRB
Independent variables	LR:UB SD:UB SA:UB BT:UB CDI:UB WS:UB RH:UB BP:UB	LR:UB SD:UB SA:UB BT:UB CDI:UB	LR:UGRB SD:UGRB SA:UGRB BT:UGRB CDI:UGRB WS:UGRB RH:UGRB BP:UGRB	LR:UGRB SD:UGRB SA:UGRB BT:UGRB CDI:UGRB WS:UGRB	LR:UGRB SD:UGRB SA:UGRB BT:UGRB CDI:UGRB
σ (ppb)	11.9	13.6	7.6	7.7	9.9
ε (ppb)	8.6	10.1	5.4	5.5	7.2
p value	–1	–1	0.5	0.5	1.75

Figure 5 plots the predicted against the measured ozone concentration for each day in the calibration set of Ouray-5. (Similar plots for all five models are given in Online Resource 3.) If the model were able to make exact predictions, then all points would of course lie on the diagonal. The standard deviations and errors for each model are given in Table 2. In any case, the agreement between actual and predicted ozone concentrations is good enough that we can make useful predictions. Agreement is especially good at lower ozone concentrations, but for reasons we do not understand, the models consistently underestimate the highest ozone concentrations. We have been able to compensate somewhat for the poorer performance at higher concentrations through the introduction of the weight factors defined in Eq. (6), so that the models predict very accurately the number of exceedance days per season.

Figure 6 show the response of Ouray-8 and Boulder-8 to variations in the independent variables. The ozone concentration as predicted by the model is plotted along the ordinate, while along the abscissa is displayed the displacement of each variable from its mean value. All curves converge at a point near the center of each graph that represents the model prediction (75.2 and 51.0 ppb, respectively) when all independent variables are held at their mean values (μ). Then, each individual curve shows how the predicted concentration varies as one of the variables is allowed to change from a low value equal to two standard deviations below its mean ($\mu - 2\sigma$) to two standard deviations above ($\mu + 2\sigma$), while holding all other variables at their means. The means (μ) and standard deviations (σ) of each variable are tabulated in Table 1. By

virtue of their definitions, CDI, WS, and SD can never be negative. Whenever $\mu - 2\sigma$ is negative for these variables, the associated curve terminates at the zero of the variable, rather than at $\mu - 2\sigma$. Because this is a quadratic regression, each of the curves in Fig. 6 is a parabola. (A linear regression would have produced straight lines.) Obviously, the variables with high sensitivity show large vertical displacements on these graphs. Table 4 shows each variable ranked according to its maximum vertical displacement in Fig. 6.

We can make all of the following observations about the curves in Fig. 6 and the sensitivities tabulated in Table 4. It should be remembered that these curves show the behavior of the models, not of the actual ozone systems of the two basins. Nevertheless, they suggest clues to the operation of the actual systems:

1. The magnitudes of the sensitivities are greater for the UB. Of the two basins, it generally forms more ozone.
2. SA is the single strongest predictor of ozone concentration in both basins. The sign of the SA correlation is appropriate, since we are measuring solar angle relative to the zenith.
3. The sensitivity of LR relative to that of other variables is smaller than we might have anticipated, since we have assumed that LR would reflect both the depth and the stability of the mixing layer. On the other hand, the data seem to indicate that in late winter, significant ozone events can occur even when the lapse rate is trending positive (Mansfield and Hall 2013). The relative sensitivities of SA and LR support this observation.

Table 3 Calibration and prediction sets of the models

	Calibration set	Prediction set
Ouray-5	239 days: mid-Dec 2009 to mid-Mar 2010; mid-Dec 2010 to mid-Mar 2011; Jan and Feb 2012	Jan 1950 to Feb 2012, but with gaps in 1950s
Ouray-8	Same as Ouray-5	Jan 2005 to Feb 2012, but with gaps
Boulder-5	594 days: early Feb 2005 to mid-Mar 2005; mid-Dec to mid-Mar for each season from 2005–2006 to 2010–2011; mid-Dec 2011 to early Feb 2012	Dec 1990 to Jan 2012, but with gaps.
Boulder-6	Same as Boulder-5	Mar 1998 to Jan 2012
Boulder-8	Same as Boulder-5	Same as Boulder-6

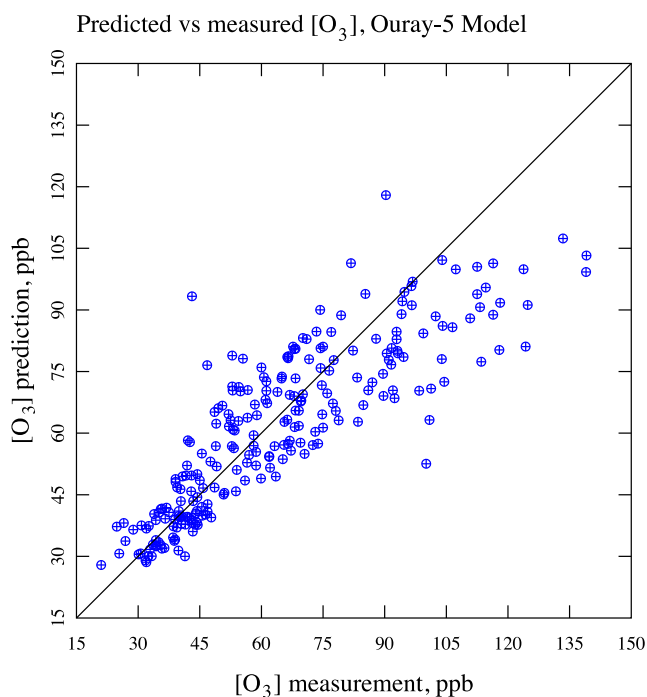


Fig. 5 Scatter plot of predicted vs. measured ozone concentrations for the Ouray-5 model

- Sensitivity to BT is relatively strong in both basins, and the associated parabolas go through a maximum very near 0 °C. In other words, ozone concentrations are positively correlated with BT below 0 °C, but switch to negative correlation above. There are at least two possible explanations for this switch. The first is that the switch is an accurate representation of the response of the ozone system to changes in temperature. Obviously, chemistry depends on temperature, but a switch from positive to negative correlation would probably require a fundamental change in the chemistry at 0 °C. Another explanation is based on the fact that our “independent” variables are not really mutually independent: For example, BT is correlated both with SA and with SD. Perhaps, the true dependence of ozone concentration on SA and/or SD cannot be adequately represented by Eq. (1), so some of that dependence “spills over” into the BT dependence. These two explanations are not mutually exclusive; both could be partly true.
- The vertices of the SD parabola in Ouray-8 and the WS parabola in Boulder-8 lie in the vicinity of $\mu + \sigma$. Rather than seeing switches from positive to negative correlation, we may be seeing saturation effects. For instance, as soon as the snow is deep enough to cover surface irregularities and vegetation, we expect the ozone system to be more or less independent of additional increases in snow depth. Equivalently, as soon as the wind speed is high enough to promote good mixing, ozone concentrations are probably insensitive to a further increase in wind speed. Any sufficiently sophisticated regression analysis might select a

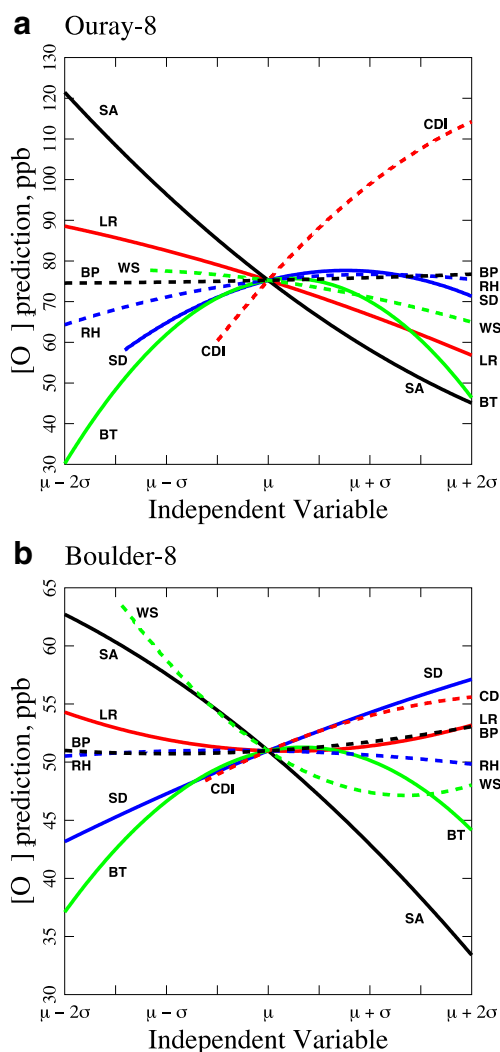


Fig. 6 Predicted ozone concentrations of the Ouray-8 model (a) and the Boulder-8 model (b). The point at the convergence of all eight traces gives the predicted concentration when all independent variables are held at their mean values (μ). Each curve shows the model prediction when each respective variable changes from two standard deviations below its mean ($\mu - 2\sigma$) to two standard deviations above ($\mu + 2\sigma$), while holding all other variables at their respective means. Because wind speed (*WS*), snow depths (*SD*), and consecutive days in inversions (*CDI*) are inherently positive, those traces terminate at the left at the zero of the variable

curve that levels off to an asymptote, if given the opportunity. However, since our construction is based on parabolas, and since there are many more points in the calibration set below $\mu + \sigma$ than above, a parabola with a vertex near $\mu + \sigma$ may be as close as we can get to a curve with an asymptote.

- WS* ranks second in sensitivity behind only *SA* in the UGRB, while in the UB, it ranks second to last. This probably reflects meteorological differences between the two basins.
- BP* was included in the models since barometric pressure influences the stability of inversions. However, it ranks very low in sensitivity in both basins.

Table 4 Sensitivities of the displayed models, defined as the maximum vertical displacement of the associated curves appearing in Fig. 6, in descending order

	Ouray-8		Boulder-8	
SA	76.4 ppb	SA	29.3 ppb	
CDI	53.9	WS	16.3	
BT	45.5	BT	14.2	
LR	31.7	SD	14.0	
SD	19.6	CDI	7.2	
RH	12.4	LR	3.3	
WS	12.3	BP	2.3	
BP	2.2	RH	1.2	

8. Ouray-8 has an especially high sensitivity to CDI. No doubt this reflects the effects of precursor buildup during multiday inversions.

As mentioned above, Ouray-5 and Boulder-6 are the models of choice. There are three arguments in favor of these selections:

1. Because of weak sensitivities to some variables, as revealed in Fig. 6 and in Table 4, Ouray-8 can tolerate the omission of RH, WS, and BP, while Boulder-8 can tolerate the omission of RH and BP, but not of WS.
2. The predictions of Ouray-5 and Boulder-6 for the number of exceedance days per season are in good agreement with the actual data.
3. The capacity of Ouray-5 and Boulder-6 to predict exceedances per season is not significantly worse than that of Ouray-8 and Boulder-8, respectively.

Data supporting the second and third arguments are presented in Online Resource 4.

Model performance, prediction mode

Figure 7 displays the predicted number of exceedances between December 15 and March 15 in the UB for each of 63 seasons since 1950. The red trace displays our prediction for the Ouray site (see “Estimates for regulatory sites” for an explanation of the green and blue traces). Several seasons in the decade of the 1950s have gaps in the available SD data. These were filled by proportionate assignment among all the missing days in a month, the estimates for such seasons are signaled by open symbols in Fig. 7a, and are more poorly constrained than the other estimates because, obviously, proportionate assignment can be a very bad approximation when gaps last for most or all of a month. [A similar figure in Mansfield and Hall (2013) is quantitatively different from Fig. 7 because that analysis counted only days in January and February.] Figure 8 displays the corresponding data for the UGRB, covering 15 years. Again, some estimates are poorly constrained because of gaps in the data. Figures 7b and 8 use open squares to show the actual number of exceedances each

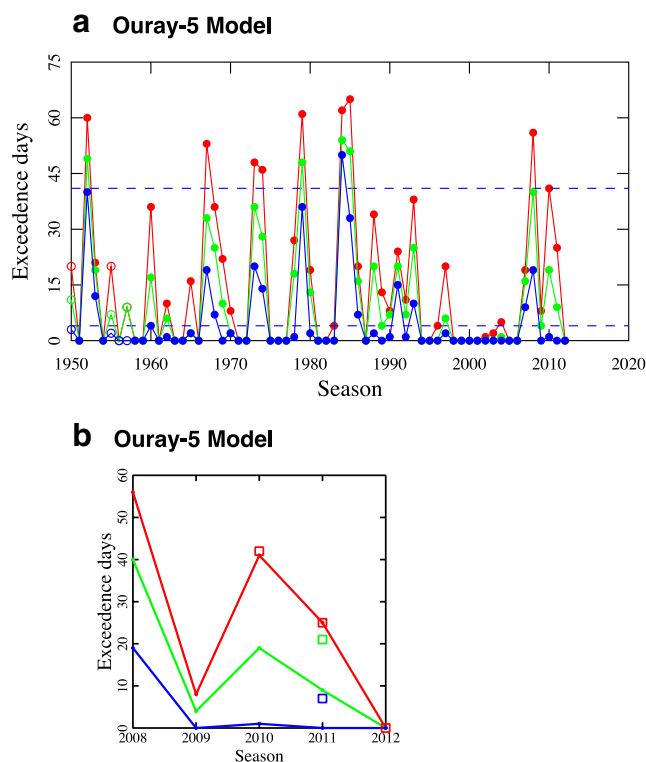


Fig. 7 Estimated number of ozone exceedances that would have occurred in the indicated season between the dates of 15 December to 15 March, if that year had precursor emissions comparable to modern values. Panel **a** shows the entire 63-year time-series, while panel **b** focuses on the most recent years. *Red traces* are the results of the Ouray-5 model. *Blue and green traces* show estimates based on a modification of the model (*Estimates for regulatory sites*) for sites at Vernal and Roosevelt, Utah, respectively. The *lower dashed line* is at 4 days; seasons below this line would have been NAAQS compliant. The *upper dashed line* is at 41 days; indicating seasons that would have been worse for ozone than 2010. *Open symbols* (at seasons 1950, 1955, 1956, and 1957) are poorly constrained estimates because of data gaps. *Open squares* display actual numbers of exceedances for the three sites: *red* Ouray, *green* Roosevelt, and *blue* Vernal

winter. (Again, see “Estimates for regulatory sites” for an explanation of the green and blue symbols.) Ozone concentrations were not measured prior to 2010 at Ouray and 2005 at Boulder. There is excellent agreement between the numbers of actual and the predicted exceedances, both at Ouray in the UB and Boulder in the UGRB, with agreement to within a single day except for Winter 2008 in the UGRB. However, this is one of the seasons that is poorly estimated because of data gaps. Thus, as long as the required input data are available, these models are accurate to ± 1 day in predicting the severity of an ozone season.

As seen in Fig. 7, $28/63=44\%$ of UB winters are predicted to have three or fewer exceedances, i.e., to be NAAQS compliant. In addition, $9/63=14\%$ of UB winters are predicted to be as bad or worse than 2009–2010, the worst season on record at the time this study was performed. Furthermore, Fig. 8 indicates that about $9/15=60\%$ of UGRB winters are predicted to be NAAQS compliant.

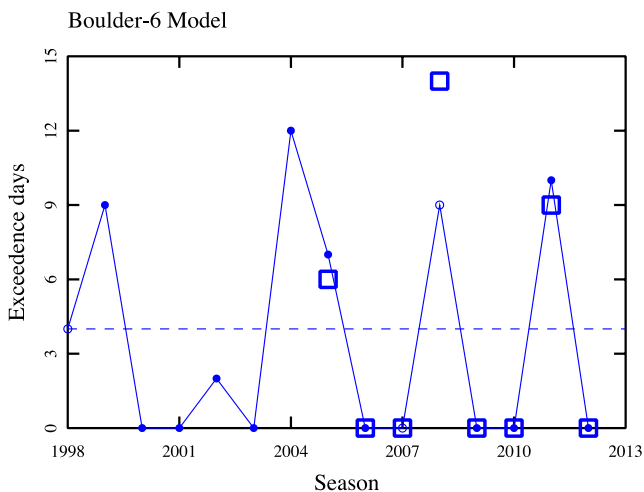


Fig. 8 Estimated number of ozone exceedances that would have occurred in the UGRB during the indicated season between the dates of 15 December to 15 March, if that season had precursor emissions comparable to modern values, as predicted by the Boulder-6 model. The dashed line is at 4 days, indicating NAAQS compliance. Open symbols (at seasons 1998, 2007, and 2008) are poorly constrained estimates because of data gaps. Open squares indicate actual numbers of exceedances

A very striking feature of the data in Fig. 7 is their broad variability. Many years are predicted to produce no exceedances, but years with 40 or more exceedances are also common. The data indicate that a typical winter pattern in the UB is the occurrence of a major snowstorm, often in December, which creates a snowpack that persists through about the end of February. The snowpack acts to stabilize inversions, setting the stage for many exceedances during the rest of the winter. On the other hand, although less typical, some winters see little or no snow, and then ozone remains close to background levels, producing no exceedances.

Figure 9 plots mean ozone concentration on any given calendar day, as predicted by either Ouray-5 or Boulder-6 and averaged over all days in the respective prediction sets. Ozone concentrations are predicted to peak in February and March in the UB and the UGRB, respectively. As indicated by Fig. 4, the likelihood of thermal inversions combined with snow cover peaks in both basins in January, but peak ozone season falls a month or two later because of the effect of solar angle.

Figure 9 also displays daily averages over the calibration sets, i.e., over days with actual ozone measurements. The two traces for the UGRB are in good agreement, primarily because the prediction set is only about twice as large as the calibration set and because the calibration set includes enough seasons, eight, that its averages are reasonably representative. Because the calibration set for the UB includes only three seasons, the agreement there is understandably poorer. In fact, with only three seasons, individual ozone events stand out as major peaks in the time series.

Mean predicted and measured ozone levels, seasonal

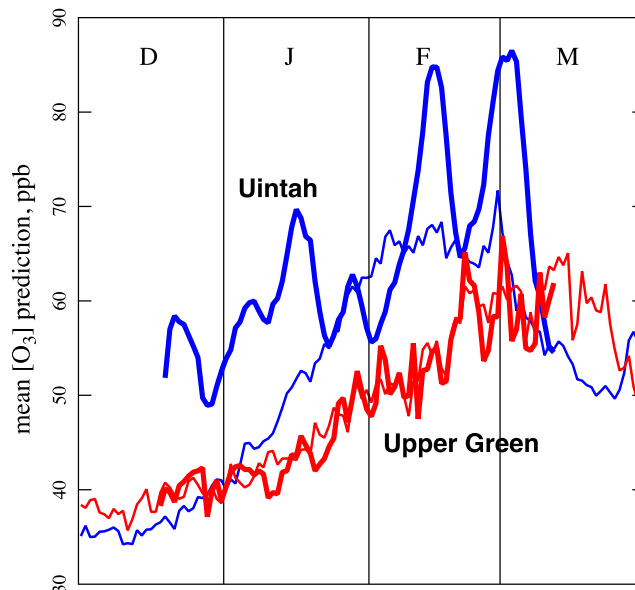


Fig. 9 Mean estimated ozone levels by day for the Ouray-5 model (blue, light) and the Boulder-6 model (red, light). Also shown are the means taken over actual measurements at Ouray (blue, heavy) and at Boulder (red, heavy). Because of excessive noise, these latter are actually displayed as 7-day running averages

Estimates for regulatory sites

As mentioned above, the Ouray site was chosen for this study because it provides the longest data sequence, covering three full winters. However, other ozone monitoring sites near the towns of Roosevelt and Vernal, Utah, will probably be used for regulatory purposes, meaning that it would be informative to make predictions for these sites as well. Figure 10 displays correlations between the 8-h daily maximum for the three sites, for one winter ozone season between 30 December 2010 and 11 March 2011. Obviously, the ozone concentration at Ouray is a good predictor of the concentrations at either Vernal or Roosevelt. If we let y_O , y_R , and y_V represent, respectively, the daily 8-h maximum in ppb at Ouray, Roosevelt, and Vernal, then the correlation lines are

$$y_R = 7.6\text{ppb} + 0.77y_O, \quad R^2 = 0.90 \tag{7}$$

$$y_V = 18.0\text{ppb} + 0.53y_O, \quad R^2 = 0.80 \tag{8}$$

We can use Eqs. (7) and (8) to estimate ozone concentrations at either Vernal or Roosevelt, given the model predictions for Ouray. The results of these estimates for exceedance days per season appear in Fig. 7. This analysis indicates that ozone concentrations are expected to be lower in Roosevelt than in Ouray and lower still in Vernal. However, Fig. 7b indicates that this approach underestimates the actual number of exceedance days in 2011.

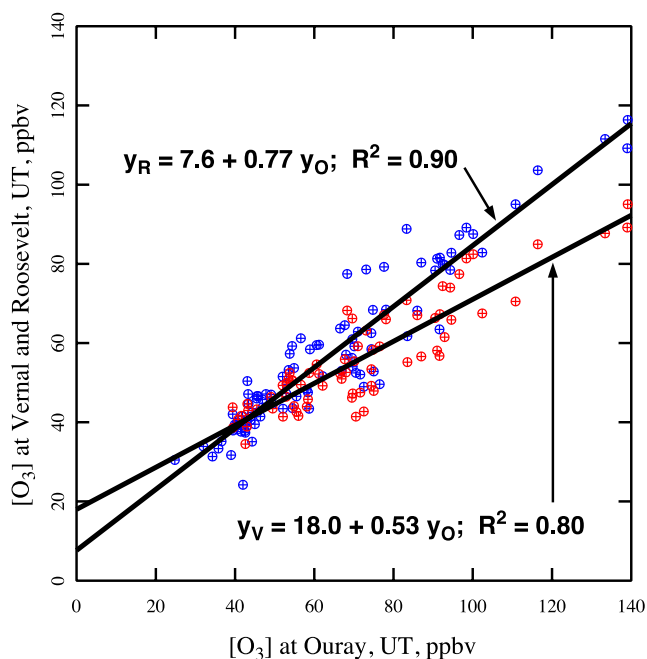


Fig. 10 Correlations between daily maxima in the 8-h average ozone concentration for the sites at Vernal, Roosevelt, and Ouray, Utah. *Red symbols* show the correlation between Vernal and Ouray, *blue* between Roosevelt and Ouray

In any case, this approach leads to the estimates that Roosevelt can be expected to be NAAQS compliant with $33/63=52\%$ odds, and Vernal with $48/63=76\%$ odds. However, based on the inability of this technique to accurately estimate the known exceedances in 2011, we caution that both of these numbers are probably overestimates. Our final projection, therefore, is that the Ouray site will be NAAQS compliant each season with about 44% odds, the Roosevelt site with odds between about 44 and 52% , and the Vernal site with odds between about 44 and 76% .

Multiyear trends and correlations in the Uinta basin ozone system

One might believe that there are nonrandom trends in the data of Fig. 7. For example, there are nine consecutive low years from 1998 to 2006, followed by five relatively high years from 2007 to 2011; there are three zero years in a row from 1975 to 1977; the two highest years—1984 and 1985—occur in succession; and from 1960 to 1984, a high ozone year occurs regularly once every 6–7 years. However, it is a common human fallacy to see nonrandomness in sequences that are essentially random (e.g., a gambler that believes he is in a winning streak). We have applied several tests for nonrandomness to the sequence of high and low years appearing in Fig. 7 and find no strong evidence for nonrandom processes. These results will be reported elsewhere.

The El Niño Southern Oscillation (ENSO), the North Atlantic Oscillation, and the Arctic Oscillation are known to exert influences on the climate of North America. Therefore, it is natural to ask whether predicted high or low ozone seasons correlate with any of these oscillations. The McVehil-Monnett study (2011) looked for correlations between ENSO and the UGRB ozone system, but found none. Likewise, elsewhere, we will report that we have been unable to find correlations between the UB ozone system and any of the above-mentioned oscillations. If any of these oscillations have a role in determining ozone behavior in the UB, it is too subtle to be detected in any of our tests.

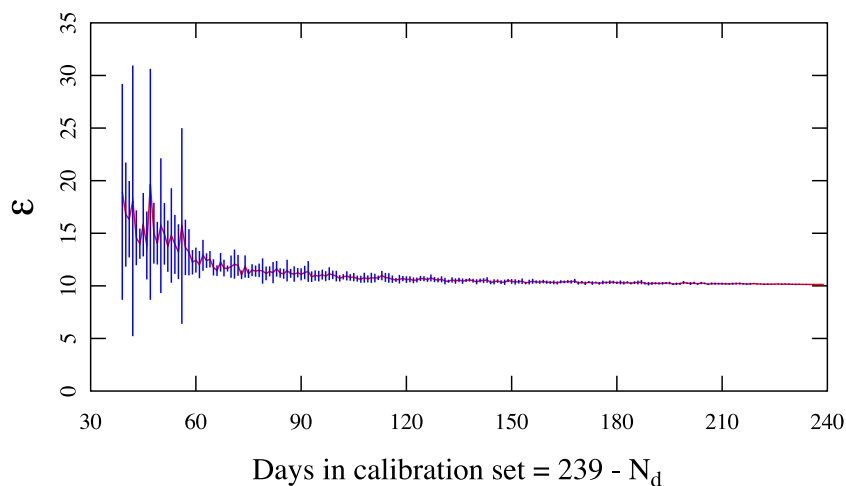
Sensitivity to data gaps

We also studied the sensitivity of the Ouray-5 model to the insertion of artificial data gaps. Of course, in the design of such models, one wants to use all available input data, but it is instructive to ask how well such models can tolerate gaps in the data, as well as how much input data is necessary for accurate model performance. We can create an artificial gap on any given day simply by setting the corresponding W_α in Eq. 2 equal to 0. Figure 11 displays the results obtained for ε (as defined in Eq. 4) when some number, N_d , of randomly selected days are discarded in this way, or equivalently, when $239-N_d$ days are retained. Ten or more independent model runs were performed at each value of N_d , and Fig. 11 displays the mean and standard deviation in ε taken over all the runs at a given value of $239-N_d$. Interestingly, if we take ε as the criterion for model performance, Fig. 11 indicates that performance does not degrade significantly until a large number of days have been discarded. When $239-N_d \approx 90$, corresponding to an omission rate of about 60% , ε is still quite close to the value of 10 obtained for the original model.

Summary, conclusions, and future work

We have developed quadratic regression models that predict the daily ozone concentration in either the Uintah Basin (UB) of Utah or the Upper Green River Basin (UGRB) of Wyoming, at ozone monitoring sites near Ouray, Utah, and Boulder, Wyoming. Input data for the Ouray-5 model, which is applicable to the UB, are daily values of lapse rate, snow depth, solar angle, temperature, and the number of consecutive days under inversion conditions. The Boulder-6 model, applicable to the UGRB, requires the same five inputs as well as the wind speed. Outputs of the models are estimates of the daily maximum in the 8-h running average ozone concentration. The regression models estimate the total number of daily exceedances of the NAAQS standard in any one season to an

Fig. 11 Sensitivity of the Ouray-5 model to artificial gaps, created by discarding N_d randomly selected days from the calibration set. The red traces are the means taken over at least ten independent runs at each value of N_d , and the vertical blue bars extend from one standard deviation below to one above



accuracy of ± 1 day, given adequate input data. Standard errors are 10 and 5 ppb for the UB and the UGRB, respectively.

We use input data as far back as 1950 for the UB and 1998 for the UGRB, and conclude that at current precursor emission rates, winter seasons will be NAAQS compliant 44 and 60 % of the time, at Ouray in the UB and at Boulder the UGRB, respectively. We predict that any given winter in the UB has 14 % odds of being more severe for ozone than the winter of 2009–2010, the most severe ozone season on record at the time this study was performed. The analysis of “[Estimates for regulatory sites](#)” also indicates that two additional sites, Vernal and Roosevelt in the UB, are expected to have a somewhat higher rate of NAAQS compliance.

According to the data, thermal inversions and snow cover are most likely in January in both basins. The frequency of days that simultaneously have inversions and snow cover is at a maximum of about 50 % in mid-January and conforms very well to a Gaussian distribution with a standard deviation of about 30 days, meaning that such days are less prevalent either in December or February.

Based on experience in both the UB and UGRB, as well as on the results of the regression model, we conclude that ozone events are most intense in February (in the UB) or March (in the UGRB), i.e., they lag behind the most intense inversions by a month or two. The most reasonable explanation for this lag is that solar radiation intensifies as the winter progresses. In fact, our models of both basins show strong sensitivity to solar elevation. Furthermore, the data appear to indicate that in late winter, high ozone can occur even during relatively weak inversions (Mansfield and Hall 2013).

We examined the feasibility of applying the model, as developed for the UB, to another basin. The Upper Snake River Valley of southwestern Idaho, centered near the city of Idaho Falls, experiences many of the same meteorological conditions as the UB or the UGRB. For example, we have been successful in calculated daily lapse rates there by the

approach discussed above, and find inversions to be common. However, so far as we have been able to determine, winter ozone concentrations have only been measured there for a single season. There also is no fossil fuel production there. In an attempt to determine the likelihood that this valley would exhibit winter ozone if it had the same precursors as the UB, we used the Ouray-5 model coefficients to predict O_3 concentrations using daily meteorological data from the Upper Snake. The result was poor, with predictions of both very high $[O_3]$, in excess of 500 ppbv, and negative $[O_3]$. Apparently, meteorological conditions differ sufficiently from one basin to the next, that a model developed for one basin is not transferable to another. Therefore, development of a regression model for the Upper Snake will only be possible after several seasons of ozone monitoring.

We have had some success with similar regression models of summertime, urban ozone events, in particular the Salt Lake Valley of central Utah, and plan to continue this work. Given our success in modeling the ozone systems of three separate basins, UB, UGRB, and Salt Lake, we are confident in the capacity of this approach to model ozone systems in general, although as mentioned above, it does not seem possible to transfer a model specific to one basin to any other.

One drawback of the model is that variables such as visibility or cloud cover are not included. Occasionally, the UB experiences extended periods of inversions combined with fog or a low ceiling. No ozone measurements have ever been made in the UB under such conditions, but it is reasonable to assume that cloud cover blocks enough sunlight to prevent significant ozone production, which would mean that our model estimates are high under such conditions.

As ozone monitoring continues in both basins, each passing year will permit us to refine the regression analysis. Eventually, it may be possible to tease out dependence on the levels of oil or gas production and, as mentioned in the preceding paragraph, on fog or cloud cover, as well.

Acknowledgments This research was funded by the Uintah Impact Mitigation Special Services District, Uintah County, Utah, USA, and by the Utah Science Technology and Research Initiative.

References

- EPA (2012) Air data. United States Environmental Protection Agency. www.epa.gov/airdata/ad_maps.html
- Finlayson-Pitts BJ, Pitts JN (2000) Chemistry of the upper and lower atmosphere. Academic, San Diego
- Mansfield M, Hall C (2013) The potential for ozone production in the Uintah Basin: a climatological analysis. In: Lyman S, Shorthill H (eds) Final report: 2012 Uintah Basin Winter Ozone and Air Quality Study. Utah State University, document no. CRD13-320.32, February 1, 2013. rd.usu.edu/files/uploads/ubos_2011-12_final_report.pdf
- Martin R, Moore K, Mansfield M, Hill S, Harper K, Shorthill (2011) Final report: Uinta Basin Winter Ozone and Air Quality Study: December 2010–March 2011. Energy Dynamics Laboratory, Utah State University Research Foundation, document no. EDL/11-039, June 14, 2011. rd.usu.edu/files/uploads/edl_2010-11_report_ozone_final.pdf
- McVehil-Monnett Associates, Inc. (2011) Ground-level ozone and meteorological parameter correlation analysis for the upper Green River Basin. Report to Wyoming Department of Environmental Quality, October 2011, MMA project no. 2451-11. www.mcvehil-monnett.com
- NOAA:NCDC (2012) National Climatic Data Center, National Oceanic and Atmospheric Administration. www.ncdc.noaa.gov/land-based-station-data/land-based-datasets
- Schnell RC, Oltmans SJ, Neeley RR, Endres MS, Molenaar JV, White AB (2009) Rapid photochemical production at high concentrations in a rural site during winter. *Nat Geosci* 2:120–122
- Seinfeld JH, Pandis SN (2006) Atmospheric chemistry and physics, 2nd edn. Wiley-Interscience, Hoboken
- Stoeckenius T, Ma L (2010) Final report: a conceptual model of winter ozone episodes in Southwest Wyoming, Environ, Novato
- Utah Climate Center (2012) Utah Climate Center, Utah State University. www.climate.usurf.usu.edu